

Title:

Toxicokinetic studies of the four new psychoactive substances 4-chloroethcathinone, N-ethylnorpentylone, N-ethylhexedrone, and 4-fluoro-alpha-pyrrolidinohexiophenone

Authors:

Lea Wagmann, Sascha K. Manier, Niels Eckstein, Hans H. Maurer & Markus R. Meyer

This is a post-peer-review, pre-copyedit version of an article published in *Forensic Toxicology* (Volume 38, Pages 59–69(2020), DOI: 10.1007/s11419-019-00487-w)

The final authenticated version is available online at: <https://doi.org/10.1007/s11419-019-00487-w>



Toxicokinetic studies of the four new psychoactive substances 4-chloroethcathinone, *N*-ethylnorpentylone, *N*-ethylhexedrone, and 4-fluoro-alpha-pyrrolidinohexiophenone

Lea Wagmann^a, Sascha K. Manier^a, Niels Eckstein^b, Hans H. Maurer^a, Markus R. Meyer^a

^a Department of Experimental and Clinical Toxicology, Institute of Experimental and Clinical Pharmacology and Toxicology, Center for Molecular Signaling (PZMS), Saarland University, Homburg, Germany

^b Department of Applied Pharmacy, University of Applied Sciences Kaiserslautern, Campus Pirmasens, Pirmasens, Germany

Contact

Markus R. Meyer, Department of Experimental and Clinical Toxicology, Institute of Experimental and Clinical Pharmacology and Toxicology, Center for Molecular Signaling (PZMS), Saarland University, Homburg, Germany

E-mail: markus.meyer@uks.eu

ABSTRACT

Purpose

The presented study aimed to elucidate the toxicokinetics of the four synthetic cathinones 4-chloroethcathinone (4-CEC), *N*-ethylnorpentylone (*N*-ethylpentylone, ephylone), *N*-ethylhexedrone (NEH), and 4-fluoro- α -pyrrolidinohexiophenone (4-fluoro- α -pyrrolidinohexanophenone, 4-F- α -PHP, 4F- α -PHP, 4F-PHP).

Methods

First, their metabolism was studied using human urine and blood samples. Analysis of specimens was performed by liquid chromatography-high resolution tandem mass spectrometry (LC-HRMS/MS) and gas chromatography-mass spectrometry (GC-MS). LC-HRMS/MS was also used to analyze in vitro incubations of the new psychoactive substances using pooled human liver S9 fraction (pS9), to identify the monooxygenases involved in the initial metabolic steps, and determination of plasma concentrations after standard addition method. Metabolic stability was tested in pooled human liver microsomes incubations analyzed by LC-ion trap MS.

Results

Using LC-HRMS/MS, in total 47 metabolites were found in patient samples and pS9 incubations. Using GC-MS, 4-CEC, ephylone, NEH, and five of their metabolites were detectable in urine. The following main phase I reactions were observed: carbonyl group reduction, *N*-deethylation, hydroxylation, lactam formation (4F-PHP), and demethylenation (ephylone). Mainly glucuronidations were observed as phase II reactions besides conjugates with the dicarboxylic acids malonic, succinic, and glutaric acid (4-CEC), sulfation, methylation (both ephylone), and *N*-acetylation (NEH). A broad range of monooxygenases was involved in the initial steps with exception of NEH (only CYP1A2 and CYP2C19). 4F-PHP had the shortest in vitro half-life (38 min) and highest intrinsic clearance ($15.7 \text{ mL} \times \text{min}^{-1} \times \text{kg}^{-1}$). Plasma concentrations ranged from 0.8 to 8.5 ng/mL.

Conclusions

Our results are expected to help toxicologists to reliably identify these substances in case of

suspected abuse and allow them a thorough risk assessment.

KEY WORDS

Drugs of abuse, NPS, novel psychoactive substances, metabolism study, toxicokinetics, screening targets

Introduction

The global new psychoactive substances (NPS) market is still characterized by the emergence of large numbers of new substances belonging to diverse chemical groups. Synthetic cathinones represent one of the largest groups and are frequently reported to the United Nations Office on Drugs and Crime (UNODC) [1]. Synthetic cathinones are chemically related to cathinone, which is a naturally occurring stimulant found in the khat plant (*Catha edulis*), and their pharmacodynamic profile is similar to that of other psychomotor stimulants including amphetamine-like monoamine releasing properties or cocaine-like blockade of monoamine reuptake [2, 3]. As most synthetic cathinones are sold as "legal highs" and not internationally controlled, they represent an ongoing issue for clinical and forensic toxicologists who must identify an unending variety of new drugs of abuse [4]. The knowledge about the toxicokinetics of NPS is essential for analytics but also for thorough risk assessment particularly if compounds are co-ingested with other NPS and/or therapeutics. In terms of cathinone abuse, the parent compound is often detectable in human specimens including urine [3], but identification of metabolites may confirm a positive screening result or allow a detection in late excretion phases.

The current study was based on specimens collected from a 41-year-old male who was admitted to the hospital displaying uncontrolled movements and aggressive behavior. The toxicological screening detected four synthetic cathinones (see Figure 1), by name 4-chloroethcathinone (4-CEC), *N*-ethylnorpentylone (*N*-ethylpentylone, ephylone), *N*-ethylhexedrone (NEH), and 4-fluoro- α -pyrrolidinohexiophenone (4-fluoro- α -pyrrolidinohexanophenone, 4-F- α -PHP, 4F-alpha-PHP, 4F-PHP) in blood and urine samples. The patient was discharged from hospital the next day due to an uneventful course. No metabolites of the detected NPS were described yet, with exception of four ephylone phase I metabolites detected in incubations with human liver microsomes (HLM) [5]. The rationale and aim of the present study was therefore to identify metabolites in patient specimens using liquid chromatography coupled to high-resolution tandem mass spectrometry (LC-HRMS/MS) and gas chromatography-mass spectrometry (GC-MS). Metabolites should be confirmed by and compared to *in vitro* incubations of the identified NPS

using pooled human liver S9 fraction (pS9). Based on these data suitable analytical targets should be recommended. The monooxygenases involved in the initial metabolic steps should be identified, plasma concentrations determined, and a metabolic stability study in pooled HLM (pHLM) conducted to expand the knowledge surrounding these synthetic cathinones' toxicokinetics.

Materials and methods

Chemicals and enzymes

4-CEC, ephylone, NEH, and 4F-PHP were obtained from an online vendor of NPS based in the Netherlands and identity as well as purity confirmed by HPLC, IR, and MS/MS. Stock solutions of the synthetic cathinones were prepared in methanol (1 mg/mL, each) and stored at -20°C until use. Trimipramine-d₃ was from LGC (Wesel, Germany), NADP⁺ from Biomol (Hamburg, Germany), isocitrate, isocitrate dehydrogenase, superoxide dismutase, 3'-phosphoadenosine-5'-phosphosulfate (PAPS), *S*-(5'-adenosyl)-L-methionine (SAM), dithiothreitol (DTT), reduced glutathione (GSH), acetyl coenzyme A (AcCoA), magnesium chloride (MgCl₂), potassium dihydrogenphosphate, dipotassium hydrogenphosphate, and Tris hydrochloride from Sigma-Aldrich (Taufkirchen, Germany). Zinc sulfate heptahydrate, acetonitrile (LC-MS grade), ammonium formate (analytical grade), formic acid (LC-MS grade), methanol (LC-MS grade), and all other chemicals and reagents (analytical grade) were obtained from VWR (Darmstadt, Germany). The baculovirus-infected insect cell microsomes (Supersomes) containing 1 nmol/mL of human cDNA-expressed CYP1A2, CYP2A6, CYP2B6, CYP2C8, CYP2C9 (2 nmol/mL), CYP2C19, CYP2D6, CYP2E1 (2 nmol/mL), CYP3A4, CYP3A5 (2 nmol/mL), or FMO3 (5 mg protein/mL), and pHLM (20 mg microsomal protein/mL, 360 pmol total CYP/mg protein, 26 individual donors), pS9 (20 mg microsomal protein/mL, 25 individual donors), UGT reaction mixture solution A (25 mM UDP-glucuronic acid), and UGT reaction mixture solution B (250 mM Tris HCl, 40 mM MgCl₂, and 125 µg/mL alamethicin) were obtained from Corning (Amsterdam, The Netherlands). After delivery, the

enzyme preparations were thawed at 37°C, aliquoted, snap-frozen in liquid nitrogen, and stored at –80°C until use.

Preparation of human biosamples

Authentic heparinized human blood plasma and human urine samples after suggested intake of drugs of abuse were submitted for clinical toxicological analysis to the authors' laboratory. The blood sample was centrifuged and plasma was separated. Plasma and urine were kept frozen (–20°C) until analysis. Human plasma (250 µL) was prepared according to Helfer et al. by precipitation with 750 µL of a zinc sulfate solution (35 mg/mL in water:methanol, 70:30, v/v) [6]. After shaking and centrifugation (18,407 x g, 2 min), the supernatant was transferred into an LC vial and injected onto the LC-HRMS/MS system. Human urine (100 µL) was prepared according to Wissenbach et al. by precipitation with 500 µL of acetonitrile [7]. After shaking and centrifugation (18,407 x g, 2 min), the supernatant was transferred into a glass vial and evaporated to dryness under a gentle stream of nitrogen at 50°C. The residue was dissolved in 50 µL of a mixture of eluent A and B (for LC-HRMS/MS, see chapter 2.7, 1:1, v/v), transferred into an LC vial, and injected onto the LC-HRMS/MS system. For analysis by GC-MS, the authors' standard liquid-liquid extraction for plasma and systematic toxicological analysis procedure for urine, consisting of hydrolysis, extraction, and microwave-assisted acetylation was used, and GC-MS standard operation conditions [8]. Briefly, a Hewlett Packard (HP, Agilent **Technologies**, Waldbronn, Germany) 5890 Series II gas chromatograph, an HP 5970 MSD mass spectrometer, a cross-linked methylsilicone capillary Optima-5 MS (12 m×0.2 mm I.D.), film thickness 0.35 µm (Macherey-Nagel, Düren, Germany) and the following conditions were used: injector port temperature, 280 °C; carrier gas, helium; flow rate 1 ml/min; column temperature, programmed from 100 to 310 °C at 30°/min, initial time 3 min, final time 5 min; electron ionization (EI) mode, ionization energy, 70 eV; ion source temperature, 200 °C; and scan rate, 1 scan/sec.

In vitro incubations for metabolism studies

As previously described by Richter et al. [9], the final incubation volume was 150 μ L. Incubations were performed using pS9 (2 mg microsomal protein/mL) after preincubation for 10 min at 37 °C with 25 μ g/mL alamethicin (UGT reaction mixture solution B), 90 mM phosphate buffer (pH 7.4), 2.5 mM Mg^{2+} , 2.5 mM isocitrate, 0.6 mM $NADP^+$, 0.8 U/mL isocitrate dehydrogenase, 100 U/mL superoxide dismutase, and 0.1 mM AcCoA. Thereafter, 2.5 mM UDP-glucuronic acid (UGT reaction mixture solution A), 40 μ M PAPS, 1.2 mM SAM, 1 mM DTT, 10 mM GSH, and 25 μ M substrate (one of the four synthetic cathinones) were added. All given concentrations correspond to the final concentrations in one reaction tube. The organic solvent content in the final incubation mixtures was always below 1% [10]. The reaction was initiated by addition of the substrate and the reaction mixture was incubated for a maximum of 360 min. After 60 min, an aliquot of 60 μ L of the incubation mixture was transferred to a reaction tube containing 20 μ L ice-cold acetonitrile for termination of the reactions. The remaining mixture was incubated for additional 300 min and thereafter stopped by addition of 30 μ L ice-cold acetonitrile. After addition of acetonitrile, mixtures were cooled for 30 min at -20°C, centrifuged (18,407 x g, 2 min), and supernatants transferred into LC vials, followed by injection onto the LC-HRMS/MS system. Blank samples without substrate and control samples without pS9 were prepared to confirm the absence of interfering compounds and identification of compounds not formed by metabolism, respectively. All incubations were performed in duplicate ($n = 2$).

Monoxygenases activity screening

According to a published procedure [11], microsomal incubations in duplicate were performed at 37 °C for 30 min using a substrate concentration of 25 μ M and CYP1A2, CYP2A6, CYP2B6, CYP2C8, CYP2C9, CYP2C19, CYP2D6, CYP2E1, CYP3A4, CYP3A5 (75 pmol/mL each), or FMO3 (0.25 mg protein/mL). Reference incubations with pHLM (1 mg microsomal protein/mL) were used as positive control. Control samples without enzymes were prepared to assess formation of compounds not originated from metabolism. Besides enzymes and substrates, the incubation mixtures (final volume, 50 μ L) contained 90 mM phosphate buffer (pH 7.4), 5 mM Mg^{2+} , 5 mM

isocitrate, 1.2 mM NADP⁺, 0.5 U/mL isocitrate dehydrogenase, and 200 U/mL superoxide dismutase. For incubations with CYP2A6 or CYP2C9, phosphate buffer was replaced with 90 mM Tris buffer, respectively, according to the manufacturer's recommendation. Reactions were initiated by addition of the enzyme preparation and terminated by addition of 50 μ L of ice-cold acetonitrile. Mixtures were centrifuged (18,407 x g, 2 min), supernatants transferred into LC vials, and injected onto the LC-HRMS/MS system.

Determination of plasma concentrations

Standard addition method was used for quantification of 4-CEC, ephylone, NEH, and 4F-PHP in the authentic human plasma sample. Briefly, 50 μ L blood plasma were precipitated with 100 μ L acetonitrile containing 0.1% formic acid. Additionally, five samples were prepared using acetonitrile containing the four synthetic cathinones resulting in final plasma concentrations of 2, 4, 6, 8, and 10 μ g/L, respectively. Ten μ L of trimipramine-d₃ in methanol (2 μ g/L final plasma concentration) were added as internal standard. After shaking and centrifugation (-10°C, 21,130 x g, 30 min), the supernatant was transferred into an LC vial and injected onto the LC-HRMS/MS system. For quantification, the ratios of the corresponding peak area of analyte and internal standard in the HR full scan were used.

Metabolic stability studies

Metabolic stability incubations were performed with pHLM in accordance to chapter 2.4 with the following variations: 2.5 μ M substrate concentrations were used and incubations stopped after 0, 30, 60, 90, 120, 150, and 180 min (4-CEC, ephylone, NEH) or 0, 15, 30, 45, 60, 75, and 90 min (4F-PHP) incubation time by addition of 50 μ L of ice-cold acetonitrile containing 1 μ M trimipramine-d₃ as internal standard. Additionally, control incubations ($n = 2$) without pHLM were prepared to assess degradation of parent compounds not originated from metabolism and stopped after 180 min (4-CEC, ephylone, NEH) or 90 min (4F-PHP). All incubations were performed in duplicate. Mixtures were centrifuged (18,407 x g, 2 min), supernatants transferred into LC vials,

and injected onto the LC-ion trap (IT) MS system. The natural logarithm of the ratios of the corresponding peak area of analyte and internal standard in the HR full scan were used to assess degradation of parent compounds. GraphPad Prism 5.00 (GraphPad Software, San Diego, USA) was used for statistical evaluation. A t-test was used to determine whether $\ln[\text{peak area ratio}]_{\text{initial}}$ values were significantly different from $\ln[\text{peak area ratio}]$ values in control incubations without pHLM using the following settings: unpaired; two-tailed; significance level, 0.05; confidence intervals, 99%.

According to Baranczewski et al. [12], the following equations were used for calculations:

$$(1) \ln[\text{peak area ratio}]_{\text{remaining}} = \ln[\text{peak area ratio}]_{\text{initial}} - k \times t \quad \text{and} \quad t_{1/2} = \frac{\ln(2)}{k}$$

$$(2) CL_{\text{int, micr}} = \frac{\ln(2)}{t_{1/2}(\text{min})} \times \frac{[V]_{\text{incubation}}(\text{mL})}{[P]_{\text{incubation}}(\text{mg})}$$

$$(3) CL_{\text{int}} = CL_{\text{int, micr}} \left(\frac{\text{mL}}{\text{min} \times \text{mg}} \right) \times \frac{[\text{Liver}](\text{g})}{[\text{BW}](\text{kg})} \times \text{SF} \left(\frac{\text{mg}}{\text{g}} \right)$$

with k = slope of the linear regression fit, $t_{1/2}$ = in vitro half-life, $CL_{\text{int, micr}}$ = microsomal intrinsic clearance, CL_{int} = intrinsic clearance, $[V]_{\text{incubation}}$ = incubation volume = 0.05, $[P]_{\text{incubation}}$ = microsomal protein amount in the incubation = 0.05, $\frac{[\text{Liver}]}{[\text{BW}]}$ = liver weight normalized by body weight [13] = 26, and SF = scaling factor microsomal protein per gram of liver [12] = 33.

LC-HRMS/MS conditions

A Thermo Fisher Scientific (TF, Dreieich, Germany) Dionex UltiMate 3000 Rapid Separation (RS) UHPLC system with a quaternary UltiMate 3000 RS pump and an HTC PAL autosampler was used and controlled by the Aria MX software. The chromatographic system was coupled to a TF Q-Exactive Focus equipped with a heated electrospray ionization II (HESI-II) source. Injection volume was 10 μL for all samples. LC and MS conditions were in accordance to Michely et al. [14] with minor modifications. Gradient elution was performed using a TF Accucore PhenylHexyl column (100 mm x 2.1 mm inner diameter, 2.6 μm particle size) at 35°C. The mobile phases consisted of 2 mM aqueous ammonium formate containing formic acid (0.1%, v/v, pH 3, eluent A)

and 2 mM ammonium formate in acetonitrile/methanol (50:50, v/v) containing formic acid (0.1%, v/v) and water (1%, v/v, eluent B). The gradient was programmed as follows: 0–1 min 1% B, 1–10 min to 99% B, 10–11.5 min hold 99% B, and 11.5–13.5 min hold 1% B, at a flow rate of 0.5 mL/min from 0 to 10 min and 0.8 mL/min from 10 to 13.5 min. The HESI-II source conditions were as follows: heater temperature, 320°C; ion transfer capillary temperature, 320°C; sheath gas, 60 arbitrary units (AU); auxiliary gas, 40 AU; spray voltage, 4.00 kV, and S-lens RF level, 50.0. Mass spectrometric analysis was performed in positive full scan mode and subsequent data-dependent acquisition (DDA) with priority to mass-to-charge ratios (m/z) of parent compounds and their expected metabolites (separate inclusion lists for 4-CEC, ephylone, NEH, and 4F-PHP). Discovery mode was chosen to ensure the recording of MS² spectra of precursor ions not in the inclusion list. The settings for full scan data acquisition were as follows: polarity, positive; resolution, 35,000; scan range, m/z 100–500; automatic gain control (AGC) target, 1e6; maximum injection time (IT), 120 ms; microscans, 1; spectrum data type, profile. The settings for the DDA mode were as follows: dd-MS², discovery; resolution, 17,500; isolation window, 1.0 m/z ; AGC target, 2e5; maximum IT, 250 ms; high collision dissociation cell with stepped normalized collision energy, 17.5, 35.0, 52.5; loop count, 3; minimum AGC target, 2.5e3 (corresponds to a signal intensity threshold of 1.0e4); exclude isotopes, on; and spectrum data type, profile. Mass calibration was performed prior to analysis according to the manufacturer's recommendations using external mass calibration. TF Xcalibur Qual Browser 4.0 software was used for data handling. The settings for automated peak integration were as follows: peak detection algorithm, ICIS; baseline window, 40; area noise factor, 5; and peak noise factor, 10.

LC-ITMS conditions

A TF LXQ linear ion trap mass spectrometer equipped with a HESI-II source and coupled to a TF Accela ultra HPLC (UHPLC) system consisting of a degasser, a quaternary pump, and an autosampler was used. Injection volume was 10 μ L for all samples. LC and MS conditions were in

accordance to Wissenbach et al. with minor modifications [7]. Gradient elution was performed on a TF Hypersil GOLD C18 column (100×2.1 mm, 1.9 μm) using 10 mM aqueous ammonium formate plus 0.1% formic acid pH 3.4 (eluent A) and acetonitrile plus 0.1% formic acid (eluent B). The flow rate was set to 0.5 mL/min, and the gradient was programmed as follows: 0–1.0 min 2% B, 1.0–3.0 min to 10% B, 3.0–5.0 min to 15% B, 5.0–7.5 min to 20% B, 7.5–10.0 min to 25% B, 10.0–11.5 min to 30% B, 11.5–13.0 min to 35% B, 13.0–14.5 min to 50% B, 14.5–16.0 min to 60% B, 16.0–19.0 min to 90% B, and 19.0–21.0 hold 90% B followed by column flushing and reequilibration. The injection volume for all samples was 10 μL each. The MS conditions were as follows: polarity, positive; sheath gas, nitrogen at flow rate of 34 AU; auxiliary gas, nitrogen at flow rate of 11 AU; vaporizer temperature, 250 °C; source voltage, 3.00 kV; ion transfer capillary temperature, 300 °C; capillary voltage, 38 V; and tube lens voltage, 110 V. AGC was set to 15,000 ions for full scan and 5,000 ions for MSⁿ. The maximum IT for full scan (MS¹ stage) was set to 100 ms, spectrum data type, profile. Collision-induced dissociation (CID)-MSⁿ experiments were performed on precursor ions selected from MS¹ using DDA: MS¹ was performed in the full scan mode (m/z 100–800). MS² and MS³ were performed in the DDA mode: four DDA MS² scan filters were chosen to provide MS² on the four most intense signals from MS¹, and additionally, eight MS³ scan filters were chosen to record MS³ on the most and second most intense signals from the MS². MS² spectra were collected with a higher priority than MS³ spectra. Normalized wideband collision energies were 35.0% for MS² and 40.0% for MS³. Other settings were as follows for MS²: minimum signal threshold, 100 counts; isolation width, 1.5 u; for MS³: minimum signal threshold, 50 counts; isolation width, 2.0 u; for both stages: activation Q, 0.25; activation time, 30 ms; and dynamic exclusion mode: repeat count, 2; repeat duration, 15 s; exclusion list size, 50; exclusion duration, 15 s.

Results and discussion

Identification of metabolites in vivo and in vitro

The phase I and II metabolites of 4-CEC, ephylone, NEH, and 4F-PHP identified in authentic human biosamples or pS9 incubations by means of LC-HRMS/MS are summarized in the Electronic Supplementary Material (ESM) in Table S1. The information whether a metabolite was detected in plasma, urine and/or the in vitro incubations can be taken from Table S2 (ESM). The precursor ion (PI) mass recorded in MS¹, characteristic fragment ions (FI) in MS², relative intensities in MS², calculated exact masses, elemental compositions, deviation of the measured from the calculated masses, and retention times (RT) are also given. Metabolites were sorted by increasing mass and RT and assigned to a unique Metabolite ID. In total, nine metabolites of 4-CEC, 17 of ephylone, 11 of NEH, and 10 of 4F-PHP were tentatively identified. Furthermore, four pairs of diastereomers were identified (M12/13, M18/19, M37/38, M48/49). Absolute peak areas of 4-CEC, ephylone, NEH, 4F-PHP, and their phase I and II metabolites in MS¹ (positive ionization mode, ESI +) derived from analyses of authentic human biosamples and pS9 incubations by LC-HRMS/MS are summarized in Table S2 (ESM). Parent compounds or metabolites identified in authentic human urine by means of GC-MS are given in Table S3 (ESM). Neither parent compound nor metabolites were detectable in the plasma sample by GC-MS.

Because the number of NPS is constantly increasing, rapid and cost-effective methods are needed to study the metabolism of these compounds in order to develop suitable toxicological screening procedures. In vitro studies for example based on pS9 incubations provide a rapid way of generating an overview of the metabolic pathways [3, 15, 9, 16]. The presence of these preliminary metabolites should further be confirmed in vivo. For this purpose, animal models such as rats, pigs, or zebrafish larvae can be used, but species differences have to be considered [17-19]. An intake by humans in the framework of a controlled trial would be the gold standard, but is considered as unethical, time-consuming, and expensive. However, in rare cases, human biosamples after intake of NPS derived from authentic cases are available as presented in this study. These specimens were kept frozen until analysis as lowered temperature was shown to enhance stability of cathinones in blood samples [20]. MS-based procedures proved to be suitable for metabolism studies due to high flexibility, sensitivity, and selectivity. Especially HR devices are promising tools for identification

of unknown compounds [21], but rather expensive and not available in every toxicological laboratory. Therefore, the detectability of the four synthetic cathinones and/or their metabolites in human biosamples by GC-MS was also investigated. For all compounds, LC-HRMS¹ data was screened for potential exact PI masses of expected metabolites in the first step. Afterwards, the fragmentation pattern in the MS² spectrum was interpreted and compared to that of the parent compound for tentative identification. Due to the high number of metabolites, the fragmentation patterns could not be discussed in detail for all metabolites and only the typical FI used for identification will be discussed. Only the calculated exact masses will be used in this chapter.

As described by Niessen and Correa [22], loss of water (-18.0106 u, H₂O) is characteristic for the fragmentation pattern of cathinones, but not pyrrolidinophenones. The spectra of 4-CEC, ephylone, NEH, and most of their metabolites contained intense FI after initial water loss, while the 4F-PHP spectrum did not contain such a FI as given in Table S1 (ESM). In case of 4-CEC (PI at *m/z* 212.0837, C₁₁H₁₅ONCl), loss of water resulted in the FI at *m/z* 194.0731 (C₁₁H₁₃NCl) and the most intense FI at *m/z* 159.1043 was formed after subsequent loss of a chlorine radical (-34.9688). Both FI were shifted by -28.0313 u (C₂H₄) in the *N*-deethyl 4-CEC (M1) spectrum. After reduction of the carbonyl group (M3), water loss resulted in the most intense FI at *m/z* 196.0888. Due to the used HR device, the PI mass of M3 (*m/z* 214.0993) could be distinguished from the ²C¹³ isotope (*m/z* 214.0903) and the Cl³⁷ isotope (*m/z* 214.0807) of 4-CEC. M3 was also detected as glucuronide (M9). Furthermore, conjugates of M1 and dicarboxylic acids, by name malonic acid, succinic acid, and glutaric acid, could be detected (M6-8). Analysis in negative ionization mode confirmed these findings (see ESM, Table S1). In rat urine, conjugates of mephedrone and methylone metabolites with succinic, glutaric, and adipic acid were previously detected [23, 24]. Nor-mephedrone succinate was also described to be present in human plasma and urine [25, 26]. However, to our knowledge, this is the first report of a synthetic cathinone metabolite bound to malonic acid and the first detection of a synthetic cathinone metabolite conjugate with glutaric acid in human urine. No dicarboxylic acid conjugates of ephylone, NEH, and 4F-PHP metabolites could be detected.

Seventeen ephylone metabolites were detected, including the four phase I metabolites previously described by Krotulski et al. [5]. However, abundances of the metabolites (see ESM, Table S2) underline the importance of the additional identification of phase II metabolites. Eleven NEH metabolites could be identified including the only *N*-acetyl metabolite in this study, *N*-deethyl *N*-acetyl NEH (M32) and 10 4F-PHP metabolites were detected. All in all, metabolic pathways were comparable to the ones described for other synthetic cathinones [4].

Four pairs of diastereomers were identified. The reduction of the carbonyl group formed two diastereomeric alcohols. Mass spectra within each pair of diastereomers were very similar as already described by Uralets et al. for other diastereomers of reduced cathinones [27]. Not always after carbonyl reduction, two diastereomers could be detected. Possible explanations could be an insufficient separation by the used LC system or stereospecific formation in varying quantities.

4-CEC, ephylone, NEH, and five metabolites were detectable in the urine sample by GC-MS (see ESM, Table S3). The low number of detected metabolites and the negative screening result in plasma was potentially caused by insufficient volatility or quantity of the analytes and sensitivity of the used GC-MS apparatus.

In order to identify suitable screening targets, absolute peak areas of 4-CEC, ephylone, NEH, 4F-PHP, and their phase I and II metabolites derived from LC-HRMS/MS analyses of authentic human biosamples and pS9 incubations are given in Table S2 (ESM). Targets detected by GC-MS are given in Table S3 (ESM). For all four synthetic cathinones, the parent compound was amongst the most abundant signals in plasma and/or urine and should therefore be included in the screening procedure. For 4-CEC, the dihydro metabolite (M3), also in combination with *N*-deethylation (M2), could be recommended as additional target for LC-, and the corresponding acetylated metabolites for GC-based screening approaches. If no conjugate cleavage is performed during sample preparation, demethylenyl ephylone glucuronide (M26), with or without methylation (M27/28), should be considered for LC-based screening, otherwise the corresponding aglyca (M15-17), also for GC-MS as acetylated compounds. Only the parent compound NEH was detectable in urine by GC-MS, while 4F-PHP was not detectable in biosamples by GC-MS at all. However, suitable

targets for LC-based screenings should be *N*-deethyl and hydroxy NEH (M29 and M33), as well as oxo 4F-PHP (M43 and M44). With exception of M43, all of these recommended targets were also detectable in the pS9 incubations and structures are given in Figure 2. As given in Table S2, a lower number of metabolites were detected in pS9 incubations in comparison to human biosamples. This was most probably caused by the lack of distribution and elimination processes in *in vitro* models, which could also lead to minor formation of metabolites in concentrations under the detection limit. Furthermore, pS9 was incubated for a maximum of 360 min, while time between intake and sampling of blood and urine may have been longer. Nevertheless, these findings are based on only one authentic case and should be considered as possible limitation.

Involvement of monooxygenases in phase I metabolic reactions

In order to identify the monooxygenases involved in the synthetic cathinones' phase I metabolic transformations, a monooxygenases activity screening was conducted consisting of incubations with one out of the ten most abundant CYP isoforms in human liver or FMO3. Incubations with pHLM were used as positive control to confirm suitable incubation conditions by metabolite formation. Results are summarized in Table 1. In case of all four synthetic cathinones, the dihydro metabolites (M3, M18, M31, M42) were only detected in pHLM incubations, but not in incubations with the recombinant monooxygenases. Therefore, the monooxygenase isoforms tested in this monooxygenases activity screening are not expected to catalyze the formation of the dihydro metabolites of 4-CEC, ephylone, NEH, and 4F-PHP. CYP2C19 was found to be involved in the formation of the *N*-deethyl metabolites of 4-CEC, ephylone, and NEH (M1, M10, M29), as well as in the *N,N*-dealkyl metabolite formation of 4F-PHP (M41). Depending on the synthetic cathinone, CYP1A2, CYP2B6, or CYP3A4 were also involved in the *N*-deethylation or *N,N*-dealkylation. Hydroxylamines were only detectable in incubations with 4-CEC (M4) and ephylone (M21) and their formation was catalyzed by CYP1A2 (only 4-CEC), CYP3A4, and FMO3. The formation of demethylenyl ephylone (M15) was catalyzed by CYP1A2, CYP2C19, and CYP2D6 and of hydroxy ephylone (M20) only by CYP3A4. Both hydroxy NEH isomers (M33, M34) were only formed in

CYP1A2 incubations. CYP1A2 also catalyzed the formation of two hydroxy 4F-PHP isomers, while CYP2C19 and CYP3A4 formed all three isomers (M45-46). Oxo 4F-PHP (M44) was formed in incubations with CYP1A2, CYP2B6, and CYP3A4.

In case of 4-CEC, ephylone, and 4F-PHP, at least four different monooxygenase isoforms were involved in the phase I metabolic transformations. Therefore, an inhibition of a single isoform in case of a drug-drug interaction or interindividual expression differences are not expected to have a significant influence on their concentrations, in contrast to NEH, where only two CYP isoforms were found to be involved in the phase I metabolic reactions. Especially an inhibition of CYP1A2 would lead to almost complete inhibition of initial metabolic steps and could therefore cause a significant increase in NEH levels and toxicity.

Determination of plasma concentrations

Standard addition method was used and the authentic plasma sample analyzed without or with addition of the four synthetic cathinones resulting in final plasma concentrations of additionally 2, 4, 6, 8, and 10 ng/mL respectively. In Figure 3, the analyte concentration is plotted versus the peak area ratio of analyte and internal standard. The data points on the y-axis represent the analyte amount in the native plasma sample and after linear regression, the following plasma concentrations were determined: 1.9 ng/mL 4-CEC, 8.5 ng/mL ephylone, 1.0 ng/mL NEH, and 0.8 ng/mL 4F-PHP. Unfortunately, dosage and time of intake were unknown. No plasma concentrations were published for 4-CEC, NEH, and 4F-PHP, so far. Published ephylone concentrations in toxicological death investigations and drugged driving casework ranged from 12 to 1,200 ng/mL [5]. Therefore, plasma concentrations determined in the presented case can be considered as low. This assumption was confirmed by the patient's health status including hospital discharge after one only day and comparison to published concentrations of other synthetic cathinones [4].

Metabolic stability in pHLM incubations

Metabolic stability in pHLM incubations is depicted in Figure 4 and in vitro half-life ($t_{1/2}$) values, calculated microsomal intrinsic clearances ($CL_{int,micr}$), and intrinsic clearances (CL_{int}) are summarized in Table 2. The shortest $t_{1/2}$ was determined for 4F-PHP with 38 min. The other compounds provided $t_{1/2}$ between 85 and 105 min. The highest CL_{int} of $15.7 \text{ mL} \times \text{min}^{-1} \times \text{kg}^{-1}$ was determined for 4F-PHP, other CL_{int} were between 5.7 and $7.0 \text{ mL} \times \text{min}^{-1} \times \text{kg}^{-1}$.

Metabolic stability was determined based on disappearance of the test compound during incubation with pHLM and expressed as $t_{1/2}$, $CL_{int,micr}$, and CL_{int} . The latter was calculated by scaling $CL_{int,micr}$ to whole liver dimensions. CL_{int} is defined as the maximum activity of the liver towards a drug in the absence of other physiological determinants such as hepatic blood flow and drug binding within the blood matrix [12]. In general, the protein concentrations should be minimized to ensure the absence of non-specific protein binding and the concentration of a test compound during the incubation should be below the Michaelis-Menten constant (K_m). As there was no information on K_m values for the tested cathinones available, a preferably low concentration was used in the assay as recommended by Baranczewski et al. [12]. Non-metabolic degradation of the synthetic cathinones could be excluded by control incubations without pHLM and subsequent t-tests that did not show a significant difference in the natural logarithms of the peak area ratios of incubations after 0 min and control incubations.

According to McNaney et al. [28], 4F-PHP could be classified as intermediate clearance compound and 4-CEC, ephylone, and NEH as low clearance compounds. The determined values were comparable to the ones published for PV8 and 4-methoxy- α -PVP [29, 30]. However, CL_{int} of synthetic cathinones were much lower than the ones determined for synthetic cannabinoid receptor agonists [31, 32].

Conclusions

In total, 47 metabolites of 4-CEC, ephylone, NEH, and 4F-PHP were identified in human biosamples and pS9 incubations including conjugates with dicarboxylic acids that were not described to be present in human urine before. Suitable targets for the development of screening

procedures were recommended. As various monooxygenases were shown to be involved in the initial metabolic steps, interactions with other drugs (of abuse) based on enzyme inhibition should be unlikely, except for NEH where only CYP1A2 and CYP2C19 were involved. Due to the health status of the patient, the determined plasma concentrations between 0.8 and 8.5 ng/mL are expected to be rather low and not life-threatening. In vitro half-life values and intrinsic clearances indicated that these synthetic cathinones can be classified as intermediate (4F-PHP) or low (4-CEC, ephylone, and NEH) clearance compounds, comparable to other synthetic cathinones' clearances. In summary, the present work clearly expanded the knowledge about the toxicokinetics of the four synthetic cathinones and may help clinical and forensic toxicologists to reliably detect these compounds in human biosamples and interpret their findings.

Electronic supplementary material

Supplementary material may be found online.

Acknowledgements

The authors like to thank Daniel Arnold, Nora Toggweiler and Armin A. Weber for their support and/or helpful discussion and Thermo Fisher Scientific for providing a seed unit of the apparatus.

Compliance with ethical standards

Conflict of interest

The authors declare that they have no conflict of interest.

Ethical approval

This article does not contain any studies with human participants or animals performed by any of the authors. The human material investigated was submitted to the authors' laboratory for regular toxicological analysis.

References

1. UNODC. World Drug Report 2018. Booklet 3. Analysis of drug markets - opioids, cocaine, cannabis, synthetic drugs. In: UNODC, editor.: United Nations publication; 2018.
2. EMCDDA. European Drug Report 2018. Publications of the European Union 2018.
3. Tyrkko E, Andersson M, Kronstrand R (2016) The Toxicology of New Psychoactive Substances: Synthetic Cathinones and Phenylethylamines. *Ther Drug Monit*; 38:190 - 216
4. Ellefsen KN, Concheiro M, Huestis MA (2016) Synthetic cathinone pharmacokinetics, analytical methods, and toxicological findings from human performance and postmortem cases. *Drug Metab Rev*; 48:237 - 65
5. Krotulski AJ, Papsun DM, De Martinis BS, Mohr ALA, Logan BK (2018) N-Ethyl Pentylone (Ephylone) Intoxications: Quantitative Confirmation and Metabolite Identification in Authentic Human Biological Specimens. *J Anal Toxicol*; 42:467 - 75
6. Helfer AG, Michely JA, Weber AA, Meyer MR, Maurer HH (2017) Liquid chromatography-high resolution-tandem mass spectrometry using Orbitrap technology for comprehensive screening to detect drugs and their metabolites in blood plasma. *Anal Chim Acta*; 965:83 - 95
7. Wissenbach DK, Meyer MR, Remane D, Philipp AA, Weber AA, Maurer HH (2011) Drugs of abuse screening in urine as part of a metabolite-based LC-MSn screening concept. *Anal Bioanal Chem*; 400:3481 - 9
8. Maurer HH, Pflieger K, Weber AA. Mass spectral data of drugs, poisons, pesticides, pollutants and their metabolites. Weinheim: Wiley-VCH; 2016.
9. Richter LHJ, Maurer HH, Meyer MR (2017) New psychoactive substances: Studies on the metabolism of XLR-11, AB-PINACA, FUB-PB-22, 4-methoxy-alpha-PVP, 25-I-NBOMe, and meclonazepam using human liver preparations in comparison to primary human hepatocytes, and human urine. *Toxicol Lett*; 280:142 - 50
10. Chauret N, Gauthier A, Nicoll-Griffith DA (1998) Effect of common organic solvents on in vitro cytochrome P450-mediated metabolic activities in human liver microsomes. *Drug Metab Dispos*; 26:1 - 4
11. Wagmann L, Meyer MR, Maurer HH (2016) What is the contribution of human FMO3 in the N-oxygenation of selected therapeutic drugs and drugs of abuse? *Toxicol Lett*; 258:55 - 70
12. Baranczewski P, Stanczak A, Sundberg K, Svensson R, Wallin A, Jansson J et al. (2006) Introduction to in vitro estimation of metabolic stability and drug interactions of new chemical entities in drug discovery and development. *Pharmacol Rep*; 58:453 - 72
13. Davies B, Morris T (1993) Physiological parameters in laboratory animals and humans. *Pharm Res*; 10:1093 - 5
14. Michely JA, Meyer MR, Maurer HH (2018) Power of Orbitrap-based LC-high resolution-MS/MS for comprehensive drug testing in urine with or without conjugate cleavage or using dried urine spots after on-spot cleavage in comparison to established LC-MS(n) or GC-MS procedures. *Drug Test Anal*; 10:158 - 63
15. Richter LHJ, Flockerzi V, Maurer HH, Meyer MR (2017) Pooled human liver preparations, HepaRG, or HepG2 cell lines for metabolism studies of new psychoactive substances? A study using MDMA, MDBD, butylone, MDPHP, MDPV, MDPB, 5-MAPB, and 5-API as examples. *J Pharm Biomed Anal*; 143:32 - 42
16. Wagmann L, Richter LHJ, Kehl T, Wack F, Bergstrand MP, Brandt SD et al. (2019) In vitro metabolic fate of nine LSD-based new psychoactive substances and their analytical detectability in different urinary screening procedures. *Anal Bioanal Chem*; doi: 10.1007/s00216-018-1558-9
17. Schaefer N, Wojtyniak JG, Kettner M, Schlote J, Laschke MW, Ewald AH et al. (2016) Pharmacokinetics of (synthetic) cannabinoids in pigs and their relevance for clinical and forensic toxicology. *Toxicol Lett*; 253:7 - 16

18. Caspar AT, Westphal F, Meyer MR, Maurer HH (2018) LC-high resolution-MS/MS for identification of 69 metabolites of the new psychoactive substance 1-(4-ethylphenyl)-N-[(2-methoxyphenyl)methyl] propane-2-amine (4-EA-NBOMe) in rat urine and human liver S9 incubates and comparison of its screening power with further MS techniques. *Anal Bioanal Chem*; 410:897 - 912
19. Richter LHJ, Herrmann J, Andreas A, Park YM, Wagmann L, Flockerzi V et al. (2019) Tools for studying the metabolism of new psychoactive substances for toxicological screening purposes - A comparative study using pooled human liver S9, HepaRG cells, and zebrafish larvae. *Toxicol Lett*; 305:73 - 80
20. Sorensen LK (2011) Determination of cathinones and related ephedrine in forensic whole-blood samples by liquid-chromatography-electrospray tandem mass spectrometry. *J Chromatogr B Analyt Technol Biomed Life Sci*; 879:727 - 36
21. Wagmann L, Maurer HH (2018) Bioanalytical Methods for New Psychoactive Substances. *Handb Exp Pharmacol*; 252:413 - 39
22. Niessen WM, Correa RA. Interpretation of MS-MS Mass Spectra of Drugs and Pesticides. Hoboken, New Jersey: John Wiley & Sons; 2016.
23. Linhart I, Himl M, Zidkova M, Balikova M, Lhotkova E, Palenicek T (2016) Metabolic profile of mephedrone: Identification of nor-mephedrone conjugates with dicarboxylic acids as a new type of xenobiotic phase II metabolites. *Toxicol Lett*; 240:114 - 21
24. Zidkova M, Linhart I, Balikova M, Himl M, Dvorackova V, Lhotkova E et al. (2018) Identification of three new phase II metabolites of a designer drug methylone formed in rats by N-demethylation followed by conjugation with dicarboxylic acids. *Xenobiotica*; 48:618 - 25
25. Pozo OJ, Ibanez M, Sancho JV, Lahoz-Beneytez J, Farre M, Papaseit E et al. (2015) Mass spectrometric evaluation of mephedrone in vivo human metabolism: identification of phase I and phase II metabolites, including a novel succinyl conjugate. *Drug Metab Dispos*; 43:248 - 57
26. Olesti E, Farre M, Papaseit E, Krotonoulas A, Pujadas M, de la Torre R et al. (2017) Pharmacokinetics of Mephedrone and Its Metabolites in Human by LC-MS/MS. *AAPS J*; 19:1767 - 78
27. Uralets V, Rana S, Morgan S, Ross W (2014) Testing for designer stimulants: metabolic profiles of 16 synthetic cathinones excreted free in human urine. *J Anal Toxicol*; 38:233-41
28. McNaney CA, Drexler DM, Hnatyshyn SY, Zvyaga TA, Knipe JO, Belcastro JV et al. (2008) An automated liquid chromatography-mass spectrometry process to determine metabolic stability half-life and intrinsic clearance of drug candidates by substrate depletion. *Assay Drug Dev Technol*; 6:121-9
29. Ellefsen KN, Wohlfarth A, Swortwood MJ, Diao X, Concheiro M, Huestis MA (2016) 4-Methoxy-alpha-PVP: in silico prediction, metabolic stability, and metabolite identification by human hepatocyte incubation and high-resolution mass spectrometry. *Forensic Toxicol*; 34:61 - 75
30. Swortwood MJ, Ellefsen KN, Wohlfarth A, Diao X, Concheiro-Guisan M, Kronstrand R et al. (2016) First metabolic profile of PV8, a novel synthetic cathinone, in human hepatocytes and urine by high-resolution mass spectrometry. *Anal Bioanal Chem*; 408:4845 - 56
31. Mardal M, Gracia-Lor E, Leibnitz S, Castiglioni S, Meyer MR (2016) Toxicokinetics of new psychoactive substances: plasma protein binding, metabolic stability, and human phase I metabolism of the synthetic cannabinoid WIN 55,212-2 studied using in vitro tools and LC-HR-MS/MS. *Drug Test Anal*; 8:1039 - 48
32. Gandhi AS, Wohlfarth A, Zhu M, Pang S, Castaneto M, Scheidweiler KB et al. (2015) High-resolution mass spectrometric metabolite profiling of a novel synthetic designer drug, N-(adamantan-1-yl)-1-(5-fluoropentyl)-1H-indole-3-carboxamide (STS-135), using cryopreserved human hepatocytes and assessment of metabolic stability with human liver microsomes. *Drug Test Anal*; 7:187 - 98

Legends to the figures

Figure 1. Chemical structures of the investigated synthetic cathinones.

Figure 2. Chemical structures of metabolites recommended as screening targets for liquid chromatography-based urine screenings.

Figure 3. Obtained standard addition calibration curves after addition of 0, 2, 4, 6, 8, or 10 ng/mL 4-CEC, ephylone, NEH, and 4F-PHP to authentic human plasma after unknown dose and time of consumption. Analyte concentration is plotted versus peak area ratios of analyte and internal standard (trimipramine-d₃).

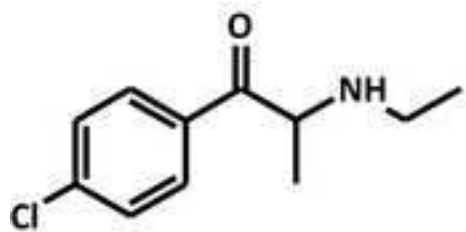
Figure 4. Metabolic stability of 4-CEC (A), ephylone (B), NEH (C), and 5F-PHP (D) in incubations with pooled human liver microsomes (pHLM). Incubation time is plotted versus the natural logarithm of the peak area ratios of the analyte and the internal standard (IS). Points indicate mean values ($n = 2$). $t_{1/2}$, in vitro half-life

Table 1. General involvement of monooxygenases in the formation of the given 4-CEC, ephylone, NEH, and 4F-PHP metabolites. Pooled human liver microsomes (pHLM) incubations were used as positive control. Metabolite IDs correspond to Table S1. CYP, cytochrome P450; FMO, flavin-containing monooxygenase, +, detected; -, not detected

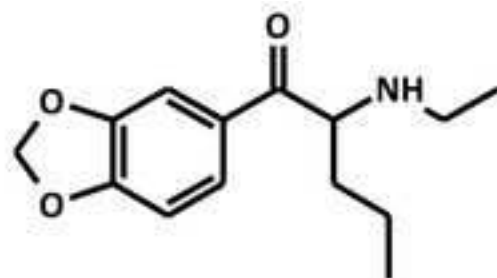
<i>Parent compound</i> Metabolite ID	CYP										FMO3	pHLM
	1A2	2A6	2B6	2C8	2C9	2C19	2D6	2E1	3A4	3A5		
<i>4-CEC</i>												
M1 (<i>N</i> -deethyl-)	+	-	+	-	-	+	-	-	-	-	-	+
M3 (dihydro-)	-	-	-	-	-	-	-	-	-	-	-	+
M4 (hydroxylamine)	+	-	-	-	-	-	-	-	+	-	+	+
<i>Ephylone</i>												
M10 (<i>N</i> -deethyl-)	-	-	+	-	-	+	-	-	+	-	-	+
M15 (demethylenyl-)	+	-	-	-	-	+	+	-	-	-	-	+
M18 (dihydro-)	-	-	-	-	-	-	-	-	-	-	-	+
M20 (hydroxy-)	-	-	-	-	-	-	-	-	+	-	-	+
M21 (hydroxylamine)	-	-	-	-	-	-	-	-	+	-	+	+
<i>NEH</i>												
M29 (<i>N</i> -deethyl-)	+	-	-	-	-	+	-	-	-	-	-	+
M31 (dihydro-)	-	-	-	-	-	-	-	-	-	-	-	+
M33 (hydroxy-)	+	-	-	-	-	-	-	-	-	-	-	+
M34 (hydroxy-)	+	-	-	-	-	-	-	-	-	-	-	+
<i>4F-PHP</i>												
M41 (<i>N,N</i> -dealkyl-)	+	-	+	-	-	+	-	-	+	-	-	+
M42 (dihydro-)	-	-	-	-	-	-	-	-	-	-	-	+
M44 (oxo-)	+	-	+	-	-	-	-	-	+	-	-	+
M45 (hydroxy-)	+	-	-	-	-	+	-	-	-	-	-	+
M46 (hydroxy-)	+	-	-	-	-	+	-	-	-	-	-	+
M47 (hydroxy-)	-	-	+	-	-	+	-	-	-	-	-	+

Table 2. Metabolic stability of 4-CEC, ephylone, NEH, and 4F-PHP in pooled human liver microsomes (pHLM) incubations expressed as in vitro half-life ($t_{1/2}$) and calculated microsomal intrinsic clearance ($CL_{int, micr}$) and intrinsic clearance (CL_{int}).

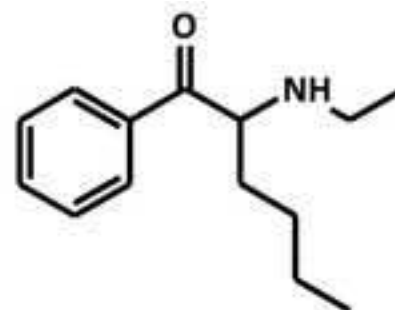
Compound	$t_{1/2}$, min	$CL_{int, micr}$, mL \times min $^{-1}\times$ mg $^{-1}$	CL_{int} , mL \times min $^{-1}\times$ kg $^{-1}$
4-CEC	105	0.0066	5.7
Ephylone	96	0.0072	6.2
NEH	85	0.0082	7.0
4F-PHP	38	0.0182	15.7



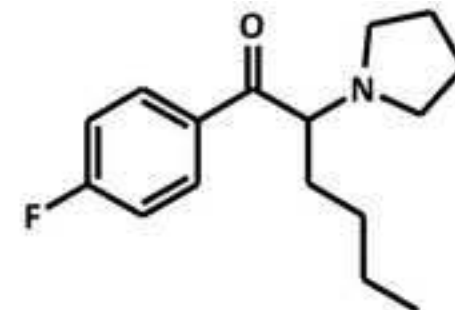
4-CEC



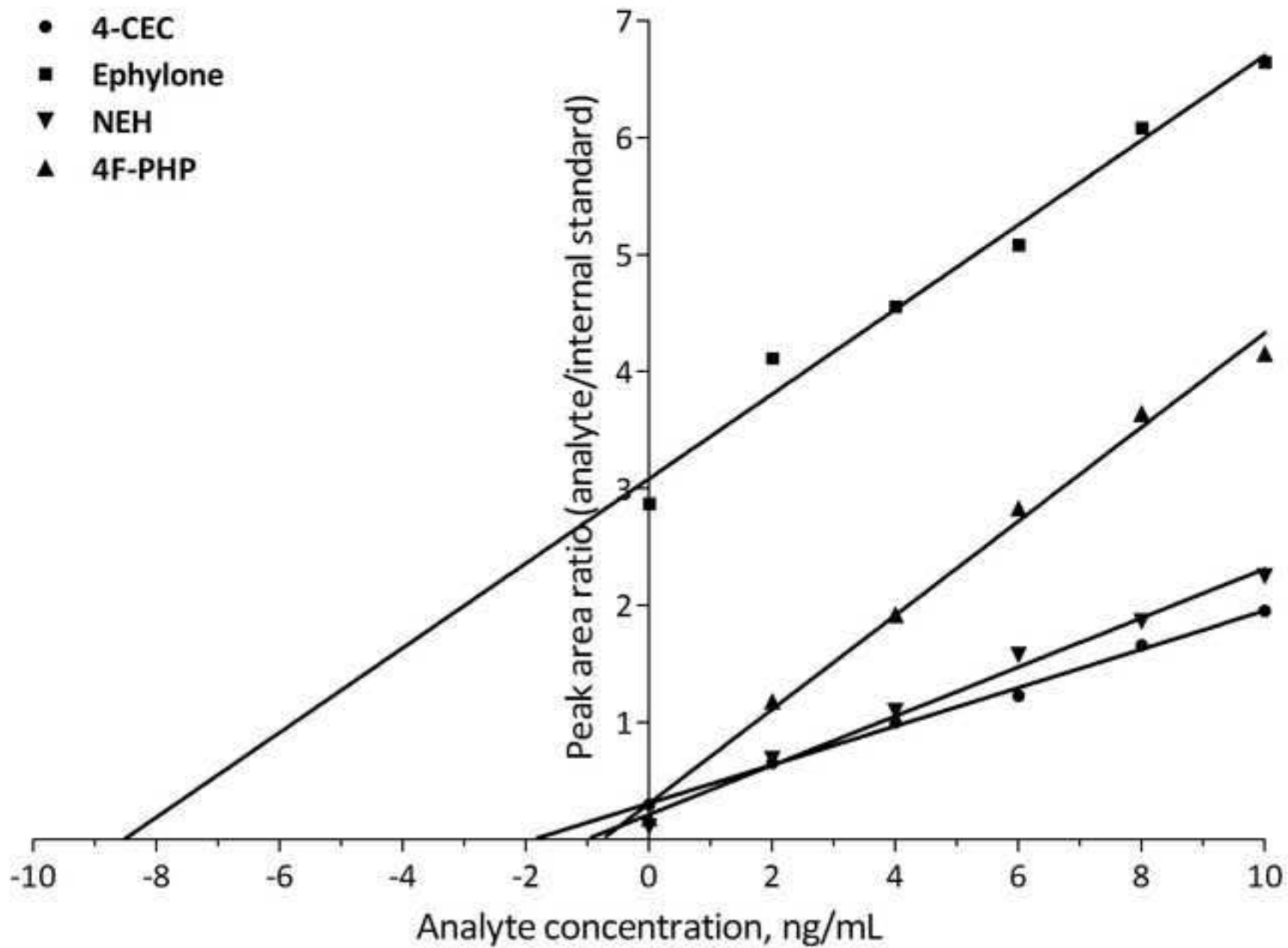
Ephylone



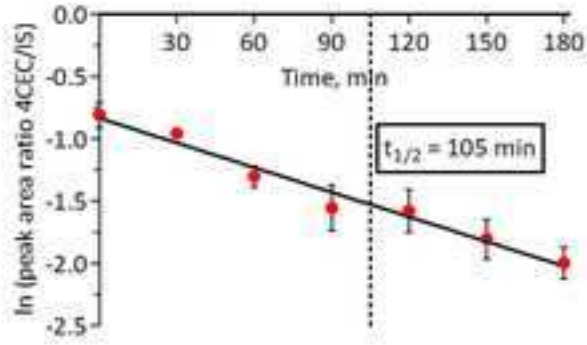
NEH



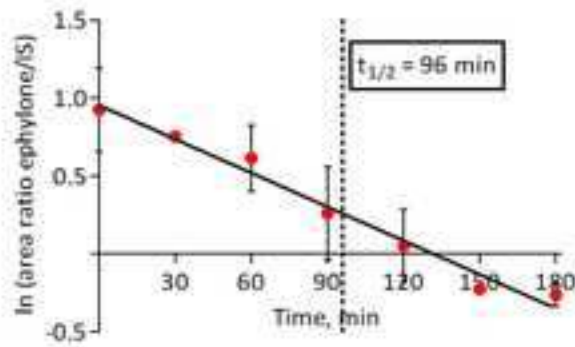
4F-PHP



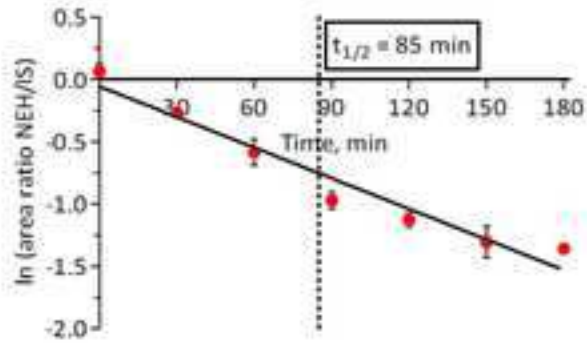
A) 4-CEC



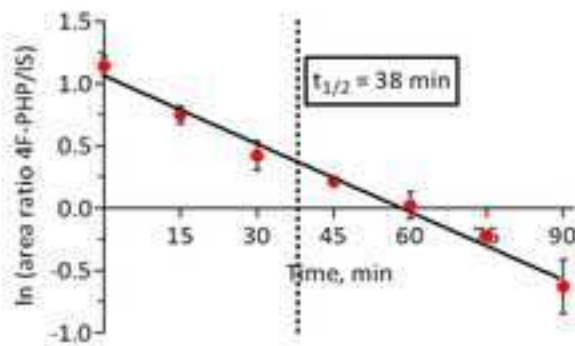
B) Ephyllone

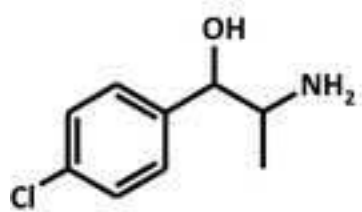


C) NEH

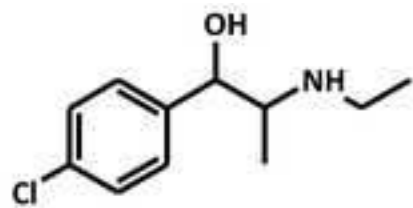


D) 4F-PHP

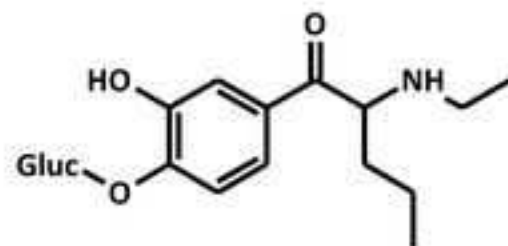




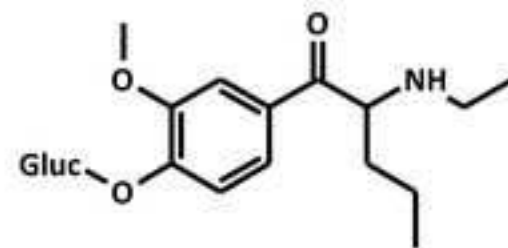
M2



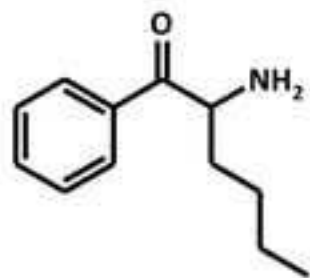
M3



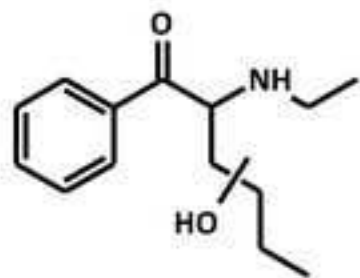
M25/26



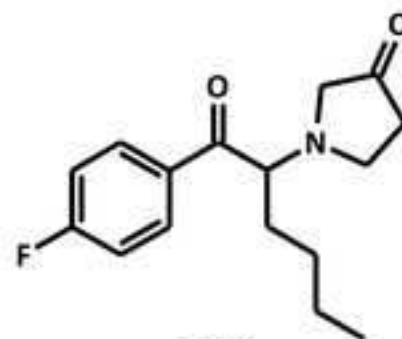
M27/28



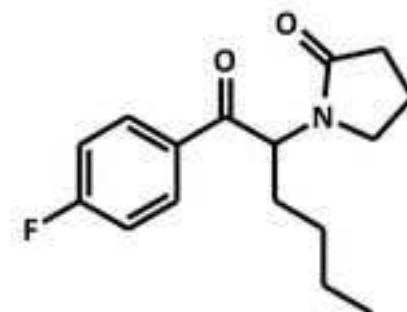
M29



M33



M43



M44

Forensic Toxicology

Electronic Supplementary Material

Toxicokinetic studies of the four new psychoactive substances 4-chloroethcathinone, *N*-ethylnorpentylone, *N*-ethylhexedrone, and 4-fluoro-alpha-pyrrolidinohexiophenone

Table S1. 4-CEC, ephylone, NEH, 4F-PHP, and their phase I and II metabolites identified in authentic human biosamples or pS9 incubations by means of LC-HRMS/MS together with the used ionization mode, precursor ion (PI) mass recorded in MS¹, characteristic fragment ions (FI) in MS², relative intensities in MS², calculated exact masses, elemental compositions, deviation of the measured from the calculated masses, and retention times (RT). Metabolites were sorted by increasing mass and RT. ESI+, positive electrospray ionization mode; ESI-, negative electrospray ionization mode

Metabolite ID	Metabolic reaction	Ionization mode	Measured masses of PI and characteristic FI, <i>m/z</i>	Relative intensity in MS ² , %	Calculated Exact Masses, <i>m/z</i>	Elemental composition	Error, ppm	RT, min
4-CEC (parent compound)	-	ESI +	PI at <i>m/z</i> 212.0837 FI at <i>m/z</i> 194.0732 FI at <i>m/z</i> 166.0417 FI at <i>m/z</i> 159.1043 FI at <i>m/z</i> 144.0808 FI at <i>m/z</i> 139.0309 FI at <i>m/z</i> 131.0731	26 86 25 100 32 15 17	212.0837 194.0731 166.0424 159.1043 144.0813 139.0309 131.0730	C ₁₁ H ₁₅ ONCl C ₁₁ H ₁₃ NCl C ₉ H ₉ NCl C ₁₁ H ₁₃ N C ₁₀ H ₁₀ N C ₈ H ₈ Cl C ₉ H ₉ N	0.00 0.52 -4.22 0.00 -3.47 0.00 0.76	3.93
M1	<i>N</i> -Deethylation	ESI +	PI at <i>m/z</i> 184.0519 FI at <i>m/z</i> 167.0258 FI at <i>m/z</i> 166.0417 FI at <i>m/z</i> 139.0307 FI at <i>m/z</i> 131.0729 FI at <i>m/z</i> 103.0546	2 9 42 19 100 7	184.0524 167.0258 166.0418 139.0309 131.0730 103.0542	C ₉ H ₁₁ ONCl C ₉ H ₈ OCl C ₉ H ₉ NCl C ₈ H ₈ Cl C ₉ H ₉ N C ₈ H ₇	-2.72 0.00 -0.60 -1.44 -0.76 3.88	3.35
M2	<i>N</i> -Deethylation + reduction	ESI +	PI at <i>m/z</i> 186.0675 FI at <i>m/z</i> 168.0566 FI at <i>m/z</i> 151.0301 FI at <i>m/z</i> 133.0880 FI at <i>m/z</i> 116.0617	1 100 29 15 32	186.0680 168.0575 151.0309 133.0886 116.0621	C ₉ H ₁₃ ONCl C ₉ H ₁₁ NCl C ₉ H ₈ Cl C ₉ H ₁₁ N C ₉ H ₈	-2.69 -5.36 -5.30 -4.51 -3.45	3.33
M3	Reduction	ESI +	PI at <i>m/z</i> 214.0990 FI at <i>m/z</i> 196.0885 FI at <i>m/z</i> 168.0571 FI at <i>m/z</i> 151.0307 FI at <i>m/z</i> 133.0886 FI at <i>m/z</i> 116.0622	2 100 8 7 2 10	214.0993 196.0888 168.0575 151.0309 133.0886 116.0621	C ₁₁ H ₁₇ ONCl C ₁₁ H ₁₅ NCl C ₉ H ₁₁ NCl C ₉ H ₈ Cl C ₉ H ₁₁ N C ₉ H ₈	-1.40 -1.53 -2.38 -1.32 0.00 0.86	4.03
M4	<i>N</i> -Oxygenation	ESI +	PI at <i>m/z</i> 228.0783 FI at <i>m/z</i> 210.0678 FI at <i>m/z</i> 175.0991 FI at <i>m/z</i> 138.9945 FI at <i>m/z</i> 131.0730	7 2 5 100 8	228.0786 210.0680 175.0992 138.9945 131.0730	C ₁₁ H ₁₅ O ₂ NCl C ₁₁ H ₁₃ ONCl C ₁₁ H ₁₃ ON C ₇ H ₄ OCl C ₉ H ₉ N	-1.32 -0.95 -0.57 0.00 0.00	5.20
M5	Carboxylation	ESI +	PI at <i>m/z</i> 242.0590 FI at <i>m/z</i> 224.0462 FI at <i>m/z</i> 196.0517 FI at <i>m/z</i> 178.0410 FI at <i>m/z</i> 168.0569 FI at <i>m/z</i> 125.0148	11 25 11 100 16 36	242.0578 224.0473 196.0524 178.0418 168.0575 125.0153	C ₁₁ H ₁₃ O ₃ NCl C ₁₁ H ₁₁ O ₂ NCl C ₁₀ H ₁₁ ONCl C ₁₀ H ₉ NCl C ₉ H ₁₁ NCl C ₇ H ₆ Cl	4.96 -4.91 -3.57 -4.49 -3.57 -4.00	3.88
M6	<i>N</i> -Deethylation + malonylation	ESI +	PI at <i>m/z</i> 270.0523 FI at <i>m/z</i> 252.0419 FI at <i>m/z</i> 210.0315 FI at <i>m/z</i> 184.0522	5 28 5 46	270.0528 252.0422 210.0316 184.0524	C ₁₂ H ₁₃ O ₄ NCl C ₁₂ H ₁₁ O ₃ NCl C ₁₀ H ₉ O ₂ NCl C ₉ H ₁₁ ONCl	-1.85 -1.19 -0.48 -1.09	5.38

	reduction diastereomer 1		FI at m/z 206.1167 FI at m/z 174.0906 FI at m/z 151.0383 FI at m/z 146.0957 FI at m/z 72.0812	24 100 5 7 22	206.1176 174.0913 151.0390 146.0964 72.0808	$C_{12}H_{16}O_2N$ $C_{11}H_{12}ON$ $C_8H_7O_3$ $C_{10}H_{12}N$ $C_4H_{10}N$	-4.37 -4.02 -4.63 -4.79 5.55	
M13	<i>N</i> -Deethylation + reduction diastereomer 2	ESI +	PI at m/z 224.1270 FI at m/z 206.1165 FI at m/z 174.0906 FI at m/z 151.0384 FI at m/z 146.0957 FI at m/z 72.0812	2 25 100 5 7 23	224.1281 206.1176 174.0913 151.0390 146.0964 72.0808	$C_{12}H_{18}O_3N$ $C_{12}H_{16}O_2N$ $C_{11}H_{12}ON$ $C_8H_7O_3$ $C_{10}H_{12}N$ $C_4H_{10}N$	-4.91 -5.34 -4.02 -3.97 -4.79 5.55	3.52
M14	<i>N</i> -Deethylation + demethylenation + methylation isomer 2	ESI +	PI at m/z 224.1270 FI at m/z 206.1164 FI at m/z 164.0698 FI at m/z 150.0543 FI at m/z 135.0434	3 100 39 3 12	224.1281 206.1176 164.0706 150.0550 135.0441	$C_{12}H_{18}O_3N$ $C_{12}H_{16}O_2N$ $C_9H_{10}O_2N$ $C_8H_8O_2N$ $C_8H_7O_2$	-4.91 -5.82 -4.88 -4.66 -5.18	3.83
M15	Demethylenation	ESI +	PI at m/z 238.1433 FI at m/z 220.1330 FI at m/z 202.1225 FI at m/z 177.0782 FI at m/z 123.0441 FI at m/z 100.1125	59 100 87 34 38 32	238.1438 220.1332 202.1226 177.0784 123.0441 100.1121	$C_{13}H_{20}O_3N$ $C_{13}H_{18}O_2N$ $C_{13}H_{16}ON$ $C_{10}H_{11}O_2N$ $C_7H_7O_2$ $C_6H_{14}N$	-2.10 -0.91 -0.49 -1.13 0.00 4.00	3.14
M16	Demethylenation + methylation isomer 1	ESI +	PI at m/z 252.1591 FI at m/z 234.1484 FI at m/z 202.1224 FI at m/z 175.0751 FI at m/z 151.0389 FI at m/z 100.1125	40 63 100 30 11 62	252.1594 234.1489 202.1226 175.0754 151.0390 100.1121	$C_{14}H_{22}O_3N$ $C_{14}H_{20}O_2N$ $C_{13}H_{16}ON$ $C_{11}H_{11}O_2$ $C_8H_7O_3$ $C_6H_{14}N$	-1.19 -2.14 -0.99 -1.71 -0.66 4.00	3.51
M17	Demethylenation + methylation isomer 2	ESI +	PI at m/z 252.1589 FI at m/z 234.1486 FI at m/z 202.1225 FI at m/z 175.0752 FI at m/z 151.0390 FI at m/z 100.1125	40 61 100 32 12 63	252.1594 234.1489 202.1226 175.0754 151.0390 100.1121	$C_{14}H_{22}O_3N$ $C_{14}H_{20}O_2N$ $C_{13}H_{16}ON$ $C_{11}H_{11}O_2$ $C_8H_7O_3$ $C_6H_{14}N$	-1.98 -1.28 -0.49 -1.14 0.00 4.00	3.81
M18	Reduction diastereomer 1	ESI +	PI at m/z 252.1604 FI at m/z 234.1484 FI at m/z 191.0937 FI at m/z 149.0596 FI at m/z 98.0968	3 100 25 1 3	252.1594 234.1489 191.0935 149.0597 98.0964	$C_{14}H_{22}O_3N$ $C_{14}H_{20}O_2N$ $C_{11}H_{13}O_2N$ $C_9H_9O_2$ $C_6H_{12}N$	3.97 -2.14 1.05 -0.67 4.08	4.38
M19	Reduction diastereomer 2	ESI +	PI at m/z 252.1589 FI at m/z 234.1479 FI at m/z 191.0932 FI at m/z 149.0591 FI at m/z 98.0964	4 100 25 1 4	252.1594 234.1489 191.0935 149.0597 98.0964	$C_{14}H_{22}O_3N$ $C_{14}H_{20}O_2N$ $C_{11}H_{13}O_2N$ $C_9H_9O_2$ $C_6H_{12}N$	-1.98 -4.27 -1.57 -4.03 0.00	4.50
M20	Hydroxylation	ESI +	PI at m/z 266.1384 FI at m/z 248.1279 FI at m/z 230.1176 FI at m/z 206.0810 FI at m/z 176.0706 FI at m/z 72.0815	100 8 31 84 30 16	266.1387 248.1281 230.1176 206.0812 176.0706 72.0808	$C_{14}H_{20}O_4N$ $C_{14}H_{18}O_3N$ $C_{14}H_{16}O_2N$ $C_{11}H_{12}O_3N$ $C_{10}H_{10}O_2N$ $C_4H_{10}N$	-1.13 -0.81 0.00 -0.97 0.00 9.71	3.68
M21	<i>N</i> -Oxygenation	ESI +	PI at m/z 266.1383 FI at m/z 248.1274 FI at m/z 176.0701 FI at m/z 149.0233 FI at m/z 121.0285 FI at m/z 116.1072	8 2 2 100 2 7	266.1387 248.1281 176.0706 149.0233 121.0284 116.1070	$C_{14}H_{20}O_4N$ $C_{14}H_{18}O_3N$ $C_{10}H_{10}O_2N$ $C_8H_5O_3$ $C_7H_5O_2$ $C_6H_{14}ON$	-1.50 -2.82 -2.84 0.00 0.83 1.72	5.52
M22	Demethylenation + sulfation isomer 1	ESI +	PI at m/z 318.0999 FI at m/z 238.1437 FI at m/z 220.1333 FI at m/z 202.1224 FI at m/z 123.0443	54 100 94 95 43	318.1006 238.1438 220.1332 202.1226 123.0441	$C_{13}H_{20}O_6NS$ $C_{13}H_{20}O_3N$ $C_{13}H_{18}O_2N$ $C_{13}H_{16}ON$ $C_7H_7O_2$	-2.20 -0.42 0.45 -0.99 1.63	3.19

			FI at <i>m/z</i> 100.1126	9	100.1121	C ₆ H ₁₄ N	4.99	
M23	Demethylenation + sulfation isomer 2	ESI +	PI at <i>m/z</i> 318.1004 FI at <i>m/z</i> 238.1438 FI at <i>m/z</i> 220.1333 FI at <i>m/z</i> 202.1225 FI at <i>m/z</i> 123.0444 FI at <i>m/z</i> 100.1124	41 89 100 65 27 25	318.1006 238.1438 220.1332 202.1226 123.0441 100.1121	C ₁₃ H ₂₀ O ₆ NS C ₁₃ H ₂₀ O ₃ N C ₁₃ H ₁₈ O ₂ N C ₁₃ H ₁₆ ON C ₇ H ₇ O ₂ C ₆ H ₁₄ N	-0.63 0.00 0.45 -0.49 2.44 3.00	3.43
M24	Demethylenation + methylation + sulfation	ESI +	PI at <i>m/z</i> 332.1154 FI at <i>m/z</i> 252.1591 FI at <i>m/z</i> 234.1486 FI at <i>m/z</i> 202.1225 FI at <i>m/z</i> 100.1125	15 92 66 100 56	332.1162 252.1594 234.1489 202.1226 100.1121	C ₁₄ H ₂₂ O ₆ NS C ₁₄ H ₂₂ O ₃ N C ₁₄ H ₂₀ O ₂ N C ₁₃ H ₁₆ ON C ₆ H ₁₄ N	-2.41 -1.19 -1.28 -0.49 4.00	3.55
M25	Demethylenation + glucuronidation isomer 1	ESI +	PI at <i>m/z</i> 414.1740 FI at <i>m/z</i> 238.1425 FI at <i>m/z</i> 220.1320 FI at <i>m/z</i> 202.1216 FI at <i>m/z</i> 123.0437 FI at <i>m/z</i> 100.1121	44 100 88 67 28 24	414.1759 238.1438 220.1332 202.1226 123.0441 100.1121	C ₁₉ H ₂₈ O ₉ N C ₁₃ H ₂₀ O ₃ N C ₁₃ H ₁₈ O ₂ N C ₁₃ H ₁₆ ON C ₇ H ₇ O ₂ C ₆ H ₁₄ N	-4.59 -5.46 -5.45 -4.95 -3.25 0.00	1.95
M26	Demethylenation + glucuronidation isomer 2	ESI +	PI at <i>m/z</i> 414.1753 FI at <i>m/z</i> 238.1434 FI at <i>m/z</i> 220.1330 FI at <i>m/z</i> 202.1225 FI at <i>m/z</i> 123.0440 FI at <i>m/z</i> 100.1125	36 64 100 66 27 56	414.1759 238.1438 220.1332 202.1226 123.0441 100.1121	C ₁₉ H ₂₈ O ₉ N C ₁₃ H ₂₀ O ₃ N C ₁₃ H ₁₈ O ₂ N C ₁₃ H ₁₆ ON C ₇ H ₇ O ₂ C ₆ H ₁₄ N	-1.45 -1.68 -0.91 -0.49 -0.81 4.00	2.92
M27	Demethylenation + methylation + glucuronidation isomer 1	ESI +	PI at <i>m/z</i> 428.1910 FI at <i>m/z</i> 252.1590 FI at <i>m/z</i> 234.1485 FI at <i>m/z</i> 202.1225 FI at <i>m/z</i> 100.1125	16 100 60 90 58	428.1915 252.1594 234.1489 202.1226 100.1121	C ₂₀ H ₃₀ O ₉ N C ₁₄ H ₂₂ O ₃ N C ₁₄ H ₂₀ O ₂ N C ₁₃ H ₁₆ ON C ₆ H ₁₄ N	-1.17 -1.59 -1.71 -0.99 4.00	2.80
M28	Demethylenation + methylation + glucuronidation isomer 2	ESI +	PI at <i>m/z</i> 428.1915 FI at <i>m/z</i> 252.1591 FI at <i>m/z</i> 234.1485 FI at <i>m/z</i> 202.1224 FI at <i>m/z</i> 100.1125	27 98 82 100 42	428.1915 252.1594 234.1489 202.1226 100.1121	C ₂₀ H ₃₀ O ₉ N C ₁₄ H ₂₂ O ₃ N C ₁₄ H ₂₀ O ₂ N C ₁₃ H ₁₆ ON C ₆ H ₁₄ N	0.00 -1.19 -1.71 -0.99 4.00	3.25
NEH (parent compound)	-	ESI +	PI at <i>m/z</i> 220.1691 FI at <i>m/z</i> 202.1587 FI at <i>m/z</i> 175.1116 FI at <i>m/z</i> 146.0962 FI at <i>m/z</i> 118.0653 FI at <i>m/z</i> 91.0547	40 100 18 73 44 82	220.1696 202.1590 175.1117 146.0964 118.0651 91.0542	C ₁₄ H ₂₂ ON C ₁₄ H ₂₀ N C ₁₂ H ₁₅ O C ₁₀ H ₁₂ N C ₈ H ₈ N C ₇ H ₇	-2.27 -1.48 -0.57 -1.37 1.69 5.49	4.89
M29	<i>N</i> -Deethylation	ESI +	PI at <i>m/z</i> 192.1380 FI at <i>m/z</i> 175.1116 FI at <i>m/z</i> 174.1275 FI at <i>m/z</i> 118.0653 FI at <i>m/z</i> 91.0547	4 20 57 100 81	192.1383 175.1117 174.1277 118.0651 91.0542	C ₁₂ H ₁₈ ON C ₁₂ H ₁₅ O C ₁₂ H ₁₆ N C ₈ H ₈ N C ₇ H ₇	-1.56 -0.57 -1.15 1.69 5.49	4.60
M30	<i>N</i> -Deethylation + reduction	ESI +	PI at <i>m/z</i> 194.1540 FI at <i>m/z</i> 176.1432 FI at <i>m/z</i> 120.0809 FI at <i>m/z</i> 91.0547	3 100 18 33	194.1539 176.1434 120.0808 91.0542	C ₁₂ H ₂₀ ON C ₁₂ H ₁₈ N C ₈ H ₁₀ N C ₇ H ₇	0.52 -1.14 0.83 5.49	4.46
M31	Reduction	ESI +	PI at <i>m/z</i> 222.1851 FI at <i>m/z</i> 204.1745 FI at <i>m/z</i> 176.1432 FI at <i>m/z</i> 147.1040 FI at <i>m/z</i> 91.0547	5 100 2 13 14	222.1852 204.1747 176.1434 147.1043 91.0542	C ₁₄ H ₂₄ ON C ₁₄ H ₂₀ N C ₁₀ H ₁₃ N C ₁₀ H ₁₃ N C ₇ H ₇	-0.45 -0.98 -1.14 -2.04 5.49	4.99
M32	<i>N</i> -Deethylation + <i>N</i> -acetylation	ESI +	PI at <i>m/z</i> 234.1496 FI at <i>m/z</i> 192.1380 FI at <i>m/z</i> 175.1117 FI at <i>m/z</i> 174.1275 FI at <i>m/z</i> 118.0653 FI at <i>m/z</i> 91.0547	2 100 60 84 64 67	234.1489 192.1383 175.1117 174.1277 118.0651 91.0542	C ₁₄ H ₂₀ O ₂ N C ₁₂ H ₁₈ ON C ₁₂ H ₁₅ O C ₁₂ H ₁₆ N C ₈ H ₈ N C ₇ H ₇	2.99 -1.56 0.00 -1.15 1.69 5.49	6.45
M33	Hydroxylation	ESI +	PI at <i>m/z</i> 236.1635	100	236.1645	C ₁₄ H ₂₂ O ₂ N	-4.23	3.70

	isomer 1		FI at <i>m/z</i> 218.1528	45	218.1539	C ₁₄ H ₂₀ ON	-5.04	
			FI at <i>m/z</i> 200.1425	20	200.1434	C ₁₄ H ₁₈ N	-4.50	
			FI at <i>m/z</i> 173.0954	38	173.0961	C ₁₂ H ₁₃ O	-4.04	
			FI at <i>m/z</i> 158.0958	88	158.0964	C ₁₁ H ₁₂ N	-3.80	
			FI at <i>m/z</i> 105.0334	12	105.0335	C ₇ H ₅ O	-0.95	
			FI at <i>m/z</i> 91.0544	30	91.0542	C ₇ H ₇	2.20	
M34	Hydroxylation isomer 2	ESI +	PI at <i>m/z</i> 236.1649	27	236.1645	C ₁₄ H ₂₂ O ₂ N	1.69	4.23
			FI at <i>m/z</i> 218.1537	100	218.1539	C ₁₄ H ₂₀ ON	-0.92	
			FI at <i>m/z</i> 191.1065	16	191.1067	C ₁₂ H ₁₅ O ₂	-1.05	
			FI at <i>m/z</i> 162.0912	38	162.0913	C ₁₀ H ₁₂ ON	-0.62	
			FI at <i>m/z</i> 107.0495	48	107.0491	C ₇ H ₇ O	3.74	
M35	Reduction + hydroxylation	ESI +	PI at <i>m/z</i> 238.1791	22	238.1802	C ₁₄ H ₂₄ O ₂ N	-4.62	3.54
			FI at <i>m/z</i> 220.1695	14	220.1696	C ₁₄ H ₂₂ ON	-0.45	
			FI at <i>m/z</i> 202.1581	8	202.1590	C ₁₄ H ₂₀ N	-4.45	
			FI at <i>m/z</i> 175.1109	31	175.1117	C ₁₂ H ₁₅ O	-4.57	
			FI at <i>m/z</i> 160.1114	8	160.1121	C ₁₁ H ₁₄ N	-4.37	
			FI at <i>m/z</i> 105.0339	1	105.0335	C ₇ H ₅ O	3.81	
			FI at <i>m/z</i> 91.0544	100	91.0542	C ₇ H ₇	5.49	
M36	Carboxylation	ESI +	PI at <i>m/z</i> 250.1435	49	250.1438	C ₁₄ H ₂₀ O ₃ N	-1.20	3.59
			FI at <i>m/z</i> 232.1332	15	232.1332	C ₁₄ H ₁₈ O ₂ N	0.00	
			FI at <i>m/z</i> 214.1227	16	214.1226	C ₁₄ H ₁₆ ON	0.47	
			FI at <i>m/z</i> 202.1229	2	202.1226	C ₁₃ H ₁₆ ON	1.48	
			FI at <i>m/z</i> 158.1176	19	158.1176	C ₈ H ₁₆ O ₂ N	0.00	
			FI at <i>m/z</i> 91.0544	100	91.0542	C ₇ H ₇	2.20	
M37	Reduction + glucuronidation diastereomer 1	ESI +	PI at <i>m/z</i> 398.2171	18	398.2173	C ₂₀ H ₃₂ O ₇ N	-0.50	4.61
			FI at <i>m/z</i> 222.1848	10	222.1852	C ₁₄ H ₂₄ ON	-1.80	
			FI at <i>m/z</i> 204.1744	100	204.1747	C ₁₄ H ₂₀ N	-1.47	
			FI at <i>m/z</i> 147.1040	13	147.1043	C ₁₀ H ₁₃ N	-2.04	
			FI at <i>m/z</i> 91.0547	9	91.0542	C ₇ H ₇	5.49	
M38	Reduction + glucuronidation diastereomer 2	ESI +	PI at <i>m/z</i> 398.2165	23	398.2173	C ₂₀ H ₃₂ O ₇ N	-2.01	4.86
			FI at <i>m/z</i> 222.1855	4	222.1852	C ₁₄ H ₂₄ ON	1.35	
			FI at <i>m/z</i> 204.1745	100	204.1747	C ₁₄ H ₂₀ N	-0.98	
			FI at <i>m/z</i> 147.1042	14	147.1043	C ₁₀ H ₁₃ N	-0.68	
			FI at <i>m/z</i> 91.0548	11	91.0542	C ₇ H ₇	6.59	
M39	Hydroxylation + glucuronidation isomer 1	ESI +	PI at <i>m/z</i> 412.1969	25	412.1966	C ₂₀ H ₃₀ O ₈ N	0.73	3.03
			FI at <i>m/z</i> 236.1642	76	236.1645	C ₁₄ H ₂₂ O ₂ N	-1.27	
			FI at <i>m/z</i> 218.1536	100	218.1539	C ₁₄ H ₂₀ ON	-1.38	
			FI at <i>m/z</i> 191.1064	7	191.1067	C ₁₂ H ₁₅ O ₂	-1.57	
			FI at <i>m/z</i> 162.0912	22	162.0913	C ₁₀ H ₁₂ ON	-0.62	
			FI at <i>m/z</i> 107.0495	39	107.0491	C ₇ H ₇ O	3.74	
M40	Hydroxylation + glucuronidation isomer 2	ESI +	PI at <i>m/z</i> 412.1949	17	412.1966	C ₂₀ H ₃₀ O ₈ N	-4.12	3.51
			FI at <i>m/z</i> 236.1633	100	236.1645	C ₁₄ H ₂₂ O ₂ N	-5.08	
			FI at <i>m/z</i> 218.1530	52	218.1539	C ₁₄ H ₂₀ ON	-4.13	
			FI at <i>m/z</i> 200.1425	6	200.1434	C ₁₄ H ₁₈ N	-4.50	
			FI at <i>m/z</i> 173.0957	4	173.0961	C ₁₂ H ₁₃ O	-2.31	
			FI at <i>m/z</i> 158.0958	25	158.0964	C ₁₁ H ₁₂ N	-3.80	
			FI at <i>m/z</i> 105.0336	4	105.0335	C ₇ H ₅ O	0.95	
			FI at <i>m/z</i> 91.0545	8	91.0542	C ₇ H ₇	3.29	
4F-PHP (parent compound)	-	ESI +	PI at <i>m/z</i> 264.1755	100	264.1758	C ₁₆ H ₂₃ ONF	-1.14	5.09
			FI at <i>m/z</i> 193.1021	12	193.1023	C ₁₂ H ₁₄ OF	-1.04	
			FI at <i>m/z</i> 140.1432	31	140.1434	C ₉ H ₁₈ N	-1.43	
			FI at <i>m/z</i> 123.0242	16	123.0241	C ₇ H ₄ OF	0.81	
			FI at <i>m/z</i> 109.0451	73	109.0448	C ₇ H ₆ F	2.75	
			FI at <i>m/z</i> 72.0815	4	72.0808	C ₄ H ₈ N	9.71	
M41	<i>N,N</i> -Dealkylation	ESI+	PI at <i>m/z</i> 210.1291	6	210.1289	C ₁₂ H ₁₇ ONF	0.95	4.74
			FI at <i>m/z</i> 193.1022	23	193.1023	C ₁₂ H ₁₄ OF	-0.52	
			FI at <i>m/z</i> 192.1180	93	192.1183	C ₁₂ H ₁₅ NF	-1.56	
			FI at <i>m/z</i> 136.0556	100	136.0557	C ₈ H ₇ NF	-0.73	
			FI at <i>m/z</i> 123.0242	16	123.0241	C ₇ H ₄ OF	0.81	
			FI at <i>m/z</i> 109.0451	91	109.0448	C ₇ H ₆ F	2.75	
M42	Reduction	ESI +	PI at <i>m/z</i> 266.1910	29	266.1915	C ₁₆ H ₂₅ ONF	-1.88	5.29

			FI at m/z 248.1807	100	248.1809	$C_{16}H_{23}NF$	-0.81	
			FI at m/z 191.1103	46	191.1105	$C_{12}H_{14}NF$	-1.05	
			FI at m/z 109.0451	9	109.0448	C_7H_6F	2.75	
			FI at m/z 72.0815	10	72.0808	$C_4H_{10}N$	9.71	
M43	Carbonylation isomer 1	ESI +	PI at m/z 278.1538	8	278.1551	$C_{16}H_{21}O_2NF$	-4.67	4.87
			FI at m/z 193.1014	33	193.1023	$C_{12}H_{14}OF$	-4.66	
			FI at m/z 123.0237	1	123.0241	C_7H_4OF	-3.25	
			FI at m/z 109.0447	100	109.0448	C_7H_6F	-0.92	
			FI at m/z 86.0602	23	86.0600	C_4H_8ON	2.32	
M44	Carbonylation isomer 2	ESI +	PI at m/z 278.1539	62	278.1551	$C_{16}H_{21}O_2NF$	-4.31	7.33
			FI at m/z 193.1015	29	193.1023	$C_{12}H_{14}OF$	-4.14	
			FI at m/z 154.1218	15	154.1226	$C_9H_{16}ON$	-5.19	
			FI at m/z 123.0237	7	123.0241	C_7H_4OF	-3.25	
			FI at m/z 109.0447	100	109.0448	C_7H_6F	-0.92	
			FI at m/z 86.0603	29	86.0600	C_4H_8ON	3.49	
M45	Hydroxylation isomer 1	ESI +	PI at m/z 280.1695	100	280.1707	$C_{16}H_{23}O_2NF$	-4.28	3.84
			FI at m/z 262.1592	22	262.1602	$C_{16}H_{21}ONF$	-3.81	
			FI at m/z 204.1174	38	204.1183	$C_{13}H_{15}NF$	-4.41	
			FI at m/z 191.0857	2	191.0867	$C_{12}H_{12}OF$	-5.23	
			FI at m/z 156.1377	2	156.1383	$C_9H_{18}ON$	-3.84	
			FI at m/z 123.0237	7	123.0241	C_7H_4OF	-3-25	
			FI at m/z 109.0446	17	109.0448	C_7H_6F	-1.83	
			FI at m/z 72.0812	19	72.0808	$C_4H_{10}N$	5.55	
M46	Hydroxylation isomer 2	ESI +	PI at m/z 280.1693	100	280.1707	$C_{16}H_{23}O_2NF$	-5.00	3.95
			FI at m/z 262.1588	15	262.1602	$C_{16}H_{21}ONF$	-5.34	
			FI at m/z 204.1172	5	204.1183	$C_{13}H_{15}NF$	-5.39	
			FI at m/z 191.0860	2	191.0867	$C_{12}H_{12}OF$	-3.66	
			FI at m/z 156.1376	4	156.1383	$C_9H_{18}ON$	-4.48	
			FI at m/z 123.0236	3	123.0241	C_7H_4OF	-4.06	
			FI at m/z 109.0447	14	109.0448	C_7H_6F	-0.92	
			FI at m/z 72.0812	22	72.0808	$C_4H_{10}N$	5.55	
M47	Hydroxylation isomer 3	ESI +	PI at m/z 280.1703	100	280.1707	$C_{16}H_{23}O_2NF$	-1.43	4.89
			FI at m/z 262.1599	8	262.1602	$C_{16}H_{21}ONF$	-1.14	
			FI at m/z 234.1653	3	234.1653	$C_{15}H_{21}NF$	0.00	
			FI at m/z 193.1022	10	193.1023	$C_{12}H_{14}OF$	-0.52	
			FI at m/z 156.1382	18	156.1383	$C_9H_{18}ON$	-0.64	
			FI at m/z 123.0242	38	123.0241	C_7H_4OF	0.81	
			FI at m/z 109.0451	67	109.0448	C_7H_6F	2.75	
			FI at m/z 70.0659	13	70.0651	C_4H_8N	11.42	
M48	Reduction + glucuronidation diastereomer 1	ESI +	PI at m/z 442.2214	21	442.2236	$C_{22}H_{33}O_7NF$	-4.97	4.88
			FI at m/z 266.1902	4	266.1915	$C_{16}H_{25}ONF$	-4.88	
			FI at m/z 248.1797	100	248.1809	$C_{16}H_{23}NF$	-4.84	
			FI at m/z 191.1094	59	191.1105	$C_{12}H_{14}NF$	-5.76	
			FI at m/z 109.0446	9	109.0448	C_7H_6F	-1.83	
			FI at m/z 72.0813	3	72.0808	$C_4H_{10}N$	6.94	
M49	Reduction + glucuronidation diastereomer 2	ESI +	PI at m/z 442.2217	34	442.2236	$C_{22}H_{33}O_7NF$	-4.30	5.04
			FI at m/z 266.1904	5	266.1915	$C_{16}H_{25}ONF$	-4.13	
			FI at m/z 248.1795	100	248.1809	$C_{16}H_{23}NF$	-5.64	
			FI at m/z 191.1095	61	191.1105	$C_{12}H_{14}NF$	-5.23	
			FI at m/z 109.0446	10	109.0448	C_7H_6F	-1.83	
			FI at m/z 72.0812	9	72.0808	$C_4H_{10}N$	5.55	
M50	Hydroxylation + glucuronidation isomer 1	ESI +	PI at m/z 456.2007	30	456.2028	$C_{22}H_{31}O_8NF$	-4.60	3.78
			FI at m/z 280.1698	100	280.1707	$C_{16}H_{23}O_2NF$	-3.21	
			FI at m/z 262.1594	18	262.1602	$C_{16}H_{21}ONF$	-3.05	
			FI at m/z 204.1179	4	204.1183	$C_{13}H_{15}NF$	-1.96	
			FI at m/z 191.0858	1	191.0867	$C_{12}H_{12}OF$	-4.71	
			FI at m/z 123.0236	4	123.0241	C_7H_4OF	-4.06	
			FI at m/z 109.0448	11	109.0448	C_7H_6F	0.00	
			FI at m/z 72.0812	22	72.0808	$C_4H_{10}N$	5.55	
M51	Hydroxylation + glucuronidation	ESI +	PI at m/z 456.2019	81	456.2028	$C_{22}H_{31}O_8NF$	-1.97	4.57
			FI at m/z 280.1704	100	280.1707	$C_{16}H_{23}O_2NF$	-1.07	

	isomer 2		FI at m/z 262.1601	23	262.1602	$C_{16}H_{21}ONF$	-0.38	
			FI at m/z 234.1663	4	234.1653	$C_{15}H_{21}NF$	4.27	
			FI at m/z 193.1030	11	193.1023	$C_{12}H_{14}OF$	3.63	
			FI at m/z 156.1382	6	156.1383	$C_9H_{18}ON$	-0.64	
			FI at m/z 123.0242	76	123.0241	C_7H_4OF	0.81	
			FI at m/z 109.0452	75	109.0448	C_7H_6F	3.67	
			FI at m/z 70.0658	26	70.0651	C_4H_8N	9.99	

Table S2. Absolute peak areas of 4-CEC, ephylone, NEH, 4F-PHP, and their phase I and II metabolites in MS¹ (ESI +) derived from analyses of authentic human biosamples and pS9 incubations by LC-HRMS/MS. Plasma sample was diluted 1:4 and urine sample concentrated 1:2 during sample preparation. The three largest peak areas of each compound and matrix are given in bold. Metabolites IDs correspond to Table S1. n.d., not detected

Metabolite ID	Metabolic reaction	Human biosamples		pS9 incubations	
		Plasma	Urine	1 hour	6 hours
4-CEC (parent compound)	-	1.28E+06	4.83E+08	3.30E+09	1.77E+09
M1	<i>N</i> -Deethylation	5.30E+05	1.85E+07	1.61E+07	2.21E+07
M2	<i>N</i> -Deethylation + reduction	1.10E+06	5.67E+08	1.06E+05	4.30E+05
M3	Reduction	3.61E+07	3.43E+09	2.45E+08	1.66E+08
M4	<i>N</i> -Oxygenation	n.d.	n.d.	1.28E+07	1.19E+07
M5	Carboxylation	n.d.	2.38E+06	n.d.	n.d.
M6	<i>N</i> -Deethylation + malonylation	n.d.	1.63E+06	n.d.	n.d.
M7	<i>N</i> -Deethylation + succinylation	n.d.	1.86E+08	n.d.	n.d.
M8	<i>N</i> -Deethylation + glutarylation	n.d.	1.64E+07	n.d.	n.d.
M9	Reduction + glucuronidation	8.58E+04	1.47E+08	n.d.	n.d.
Ephylone (parent compound)	-	7.37E+06	8.35E+08	6.91E+09	3.98E+09
M10	<i>N</i> -Deethylation	8.83E+05	7.50E+07	3.25E+07	4.97E+07
M11	<i>N</i> -Deethylation + demethylenation + methylation isomer 1	n.d.	3.48E+07	n.d.	n.d.
M12	<i>N</i> -Deethylation + reduction diastereomer 1	n.d.	8.46E+07	n.d.	n.d.
M13	<i>N</i> -Deethylation + reduction diastereomer 2	n.d.	2.52E+07	n.d.	n.d.
M14	<i>N</i> -Deethylation + demethylenation + methylation isomer 2	n.d.	3.07E+07	n.d.	n.d.
M15	Demethylenation	5.65E+05	8.10E+07	2.25E+07	1.09E+07
M16	Demethylenation + methylation isomer 1	6.07E+05	2.42E+08	2.85E+07	2.43E+08
M17	Demethylenation + methylation isomer 2	1.82E+05	7.24E+07	1.26E+08	8.07E+07
M18	Reduction diastereomer 1	3.18E+05	5.69E+07	4.90E+07	2.87E+07
M19	Reduction	n.d.	6.56E+07	n.d.	n.d.

	diastereomer 2				
M20	Hydroxylation	n.d.	3.68E+06	4.84E+05	1.18E+06
M21	<i>N</i> -Oxygenation	n.d.	n.d.	7.84E+06	8.06E+06
M22	Demethylenation + sulfation isomer 1	n.d.	4.94E+06	4.01E+05	9.27E+05
M23	Demethylenation + sulfation isomer 2	n.d.	4.38E+06	3.68E+05	8.81E+05
M24	Demethylenation + methylation + sulfation	n.d.	1.07E+07	4.71E+06	1.58E+07
M25	Demethylenation + glucuronidation isomer 1	n.d.	1.09E+07	n.d.	n.d.
M26	Demethylenation + glucuronidation isomer 2	2.47E+06	2.98E+08	3.10E+06	2.05E+06
M27	Demethylenation + methylation + glucuronidation isomer 1	1.46E+06	2.46E+08	1.90E+07	4.04E+07
M28	Demethylenation + methylation + glucuronidation isomer 2	8.15E+05	1.76E+08	1.06E+07	1.12E+07
NEH (parent compound)	-	8.86E+05	1.16E+08	4.45E+09	2.29E +09
M29	<i>N</i> -Deethylation	7.71E+05	7.29E+07	1.74E+08	2.40E+08
M30	<i>N</i> -Deethylation + reduction	6.17E+05	6.18E+07	1.33E+07	9.38E+06
M31	Reduction	1.65E+05	5.28E+07	2.23E+08	1.33E+08
M32	<i>N</i> -Deethylation + <i>N</i> -acetylation	n.d.	n.d.	1.36E+06	1.31E+06
M33	Hydroxylation isomer 1	6.56E+05	2.02E+08	4.61E+07	6.79E+07
M34	Hydroxylation isomer 2	n.d.	3.83E+06	9.25E+06	8.33E+06
M35	Reduction + hydroxylation	n.d.	3.10E+07	n.d.	n.d.
M36	Carboxylation	n.d.	3.91E+07	n.d.	3.23E+05
M37	Reduction + glucuronidation diastereomer 1	n.d.	3.54E+07	n.d.	1.27E+05
M38	Reduction + glucuronidation diastereomer 2	n.d.	2.59E+07	n.d.	2.67E+04
M39	Hydroxylation + glucuronidation isomer 1	n.d.	1.43E+06	n.d.	3.53E+05
M40	Hydroxylation + glucuronidation isomer 2	n.d.	5.20E+06	n.d.	n.d.
4F-PHP (parent compound)	-	1.16E+06	5.41E+07	7.47E+09	4.71E+09
M41	<i>N</i> -Dealkylation	n.d.	3.05E+06	4.11E+06	5.01E+06
M42	Reduction	3.23E+06	4.17E+07	6.55E+08	4.92E+08

M43	Carbonylation isomer 1	9.62E+05	7.29E+07	n.d.	n.d.
M44	Carbonylation isomer 2	2.76E+05	6.68E+07	5.15E+07	5.10E+07
M45	Hydroxylation isomer 1	n.d.	4.45E+06	8.01E+06	1.59E+07
M46	Hydroxylation isomer 2	n.d.	6.53E+06	5.66E+06	1.08E+07
M47	Hydroxylation isomer 3	n.d.	n.d.	6.78E+07	1.11E+08
M48	Reduction + glucuronidation diastereomer 1	n.d.	7.57E+06	n.d.	n.d.
M49	Reduction + glucuronidation diastereomer 2	n.d.	8.71E+07	2.08E+05	3.12E+05
M50	Hydroxylation + glucuronidation isomer 1	n.d.	2.79E+06	n.d.	n.d.
M51	Hydroxylation + glucuronidation isomer 2	n.d.	1.51E+07	8.17E+05	1.93E+06

Table S3. Targets identified in authentic human urine by means of GC-MS. Metabolites IDs correspond to Table S1. AC, acetylated

Metabolite ID	Target	Precursor ion mass, <i>m/z</i>	Fragment ion masses, <i>m/z</i>	Retention index
Parent compound	4-CEC AC	253	72, 111, 114, 139	1920
M2	<i>N</i> -Deethyl dihydro 4-CEC 2AC	269	72, 111, 114, 141	1995
M3	Dihydro 4-CEC 2AC	297	86, 111, 141	2100
Parent compound	Ephylone AC	291	100, 121, 142, 149	2275
M11/14	<i>N</i> -Deethyl-demethylenyl-methyl ephylone AC	265	72, 114, 151	2230
M11/14	<i>N</i> -Deethyl-demethylenyl-methyl ephylone 2AC	307	72, 114, 151, 193, 265	2300
M16/17	Demethylenyl-methyl ephylone AC	293	100, 123, 142, 151	2265
M16/17	Demethylenyl-methyl ephylone isomer 1 2AC	335	100, 123, 142, 151	2355
M16/17	Demethylenyl-methyl ephylone isomer 2 2AC	335	100, 123, 142, 151	2395
Parent compound	NEH AC	261	77, 105, 114, 156	2030